

## Original Article

# Extracorporeal shock wave markedly alleviates radiation-induced chronic cystitis in rat

Yen-Ta Chen<sup>1,11</sup>, Kuan-Hung Chen<sup>4,11</sup>, Pei-Hsun Sung<sup>5,11</sup>, Chih-Chao Yang<sup>6</sup>, Ben-Chung Cheng<sup>6</sup>, Chih-Hung Chen<sup>7</sup>, Chia-Lo Chang<sup>2</sup>, Jiunn-Jye Sheu<sup>3,11</sup>, Fan-Yen Lee<sup>3,11,13</sup>, Pei-Lin Shao<sup>8</sup>, Cheuk-Kwan Sun<sup>9</sup>, Hon-Kan Yip<sup>5,8,10,11,12</sup>

<sup>1</sup>Division of Urology, Department of Surgery, Kaohsiung Chang Gung Memorial Hospital and Chang Gung University College of Medicine, Kaohsiung 83301, Taiwan; <sup>2</sup>Department of Anesthesiology, Kaohsiung Chang Gung Memorial Hospital and Chang Gung University College of Medicine, Kaohsiung 83301, Taiwan; <sup>3</sup>Division of Cardiology, Department of Internal Medicine, Kaohsiung Chang Gung Memorial Hospital and Chang Gung University College of Medicine, Kaohsiung 83301, Taiwan; <sup>4</sup>Division of Nephrology, Department of Internal Medicine, Kaohsiung Chang Gung Memorial Hospital and Chang Gung University College of Medicine, Kaohsiung 83301, Taiwan; <sup>5</sup>Divisions of General Medicine, Department of Internal Medicine, Kaohsiung Chang Gung Memorial Hospital and Chang Gung University College of Medicine, Kaohsiung 83301, Taiwan; <sup>6</sup>Division of Colorectal Surgery, Department of Surgery, Kaohsiung Chang Gung Memorial Hospital and Chang Gung University College of Medicine, Kaohsiung 83301, Taiwan; <sup>7</sup>Division of Thoracic and Cardiovascular Surgery, Department of Surgery, Kaohsiung Chang Gung Memorial Hospital and Chang Gung University College of Medicine, Kaohsiung, 83301, Taiwan; <sup>8</sup>Department of Nursing, Asia University, Taichung 41354, Taiwan; <sup>9</sup>Department of Emergency Medicine, E-Da Hospital, I-Shou University School of Medicine for International Students, Kaohsiung 82445, Taiwan; <sup>10</sup>Institute for Translational Research in Biomedicine, Kaohsiung Chang Gung Memorial Hospital, Kaohsiung 83301, Taiwan; <sup>11</sup>Center for Shockwave Medicine and Tissue Engineering, Kaohsiung Chang Gung Memorial Hospital, Kaohsiung 83301, Taiwan; <sup>12</sup>Department of Medical Research, China Medical University Hospital, China Medical University, Taichung 40402, Taiwan; <sup>13</sup>Division of Cardiovascular Surgery, Department of Surgery, Tri-Service General Hospital, National Defense Medical Center, Taipei 11490, Taiwan

Received January 17, 2018; Accepted March 4, 2018; Epub March 15, 2018; Published March 30, 2018

**Abstract:** This study tested the hypothesis that extracorporeal shock wave (ECSW) treatment can effectively inhibit radiation-induced chronic cystitis (CC). Adult male Sprague-Dawley (SD) rats (n = 24) were randomly divided into group 1 (normal control), group 2 (CC induced by radiation with 300 cGy twice with a four-hour interval to the urinary bladder), group 3 [CC with ECSW treatment (0.2 mJ/mm<sup>2</sup>/120 impulses/at days 1, 7, and 14 after radiation)]. Bladder specimens were harvested by day 28 after radiation. By day 28 after radiation, the degree of detrusor contraction impairment was significantly higher in group 2 than that in groups 1 and 3, and significantly higher in group 3 than that in group 1 (P<0.0001). The urine albumin concentration expressed an opposite pattern compared to that of detrusor function among the three groups (P<0.0001). The bladder protein expressions of inflammatory (TLR-2/TLR-4/IL-6/IL-12/MMP-9/TNF- $\alpha$ /NF- $\kappa$ B/RANTES/iNOS) and oxidative-stress (NOX-1/NOX-2/oxidized protein) biomarkers exhibited a pattern identical to that of urine albumin in all groups (all P<0.0001). The cellular expressions of inflammatory (CD14+/CD68+/CD74+/COX-2/MIF+/substance P+) and cytokeratin (CK13+/HMW CK+/CK+17/CK+18/CK+19) biomarkers, and collagen-deposition/fibrotic areas as well as epithelial-damaged score displayed an identical pattern compared to that of urine albumin among the three groups (all P<0.0001). In conclusion, ECSW treatment effectively protected urinary bladder from radiation-induced CC.

**Keywords:** Chronic cystitis, radiotherapy, extracorporeal shock wave, inflammation, oxidative stress

## Introduction

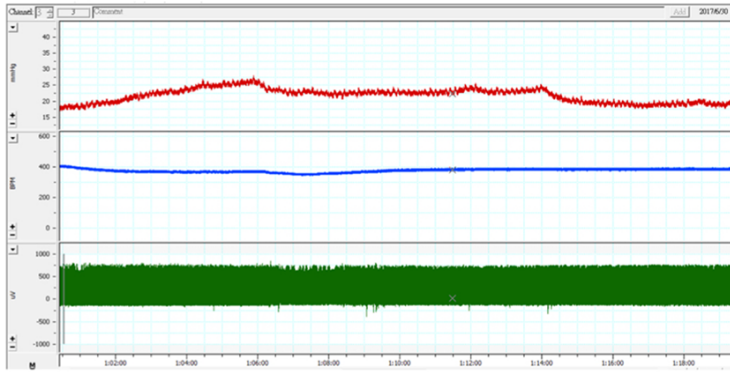
In treating patients with malignancy, chemotherapy and radiotherapy are still popular options for advanced disease [1] such as urogenital/gynecologic cancers. On the other hand, chemotherapeutic agents (e.g., cyclophosphamide) and radiotherapy frequently induce hem-

orrhagic cystitis and gross hematuria which not only impair the patient's quality of life, but also induce obstructive uropathy and renal failure as well as increase the risk of mortality [2-7].

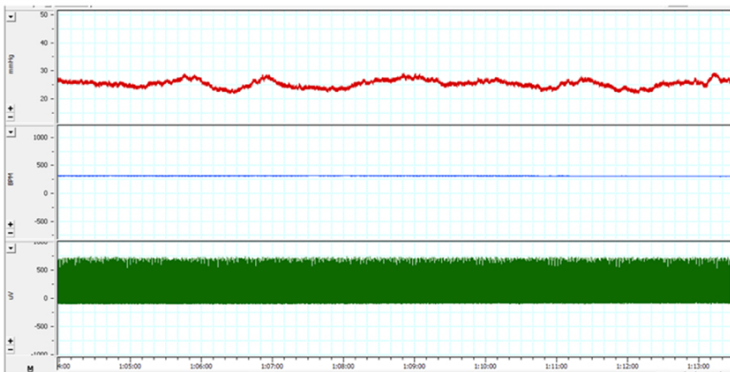
Since hemorrhagic cystitis is refractory to therapeutic agents including transamin, pentosan, prostaglandins as well as treatment strategies

# ECSW against radiation-induced chronic cystitis

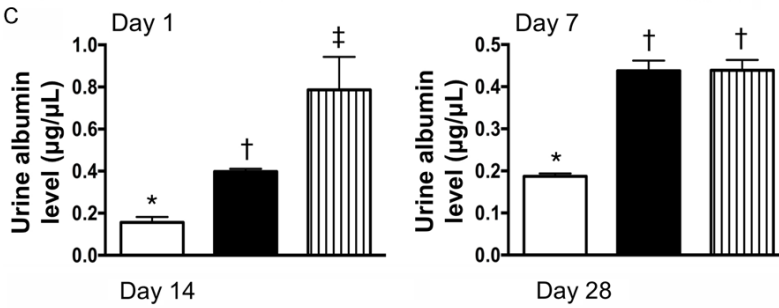
**A NC**



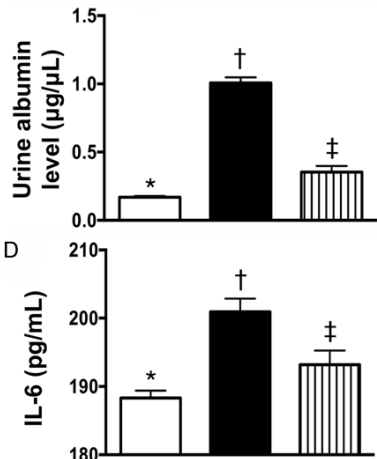
**B CC + ECSW**



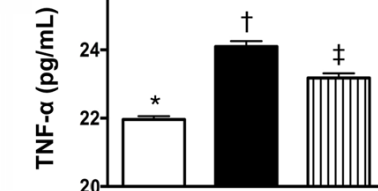
**C**



**D**



**E**



□ NC    ■ CC    ▨ CC+ECSW

such as injection of botulinum toxin A in bladder wall, intravesical instillation of aluminum, selective embolization or ligation of the internal iliac arteries, surgical or percutaneous nephrostomy with or without cystectomy, and hyperbaric oxygen therapy [8-19], treatment of chemotherapy/radiotherapy-induced hemorrhagic cystitis and its complications remains a formidable challenge. A new, safe, and efficacious treatment alternative is still eagerly awaited.

Considering the pathophysiology of radiation cystitis that involves the activation of an inflammatory cascade leading to tissue edema, mucosa damage and smooth muscle destruction, targeting the inflammatory reactions may be another therapeutic option for patients with the disease refractory to conventional treatment.

Recent studies have shown that extracorporeal shock wave (ECSW) could suppress inflammation, upregulate endogenous nitric oxide production, and enhance angiogenesis [20-22]. Additionally, our previous studies not only have established the safety of ECSW treatment, but have also demonstrated the pro-angiogenic, anti-ischemic, anti-oxidative, anti-inflammatory, and pain-alleviating effects of ECSW [20, 22-28]. Accordingly, using an animal model, we tested whether ECSW therapy would effectively ameliorate radiation-induced chronic

# ECSW against radiation-induced chronic cystitis

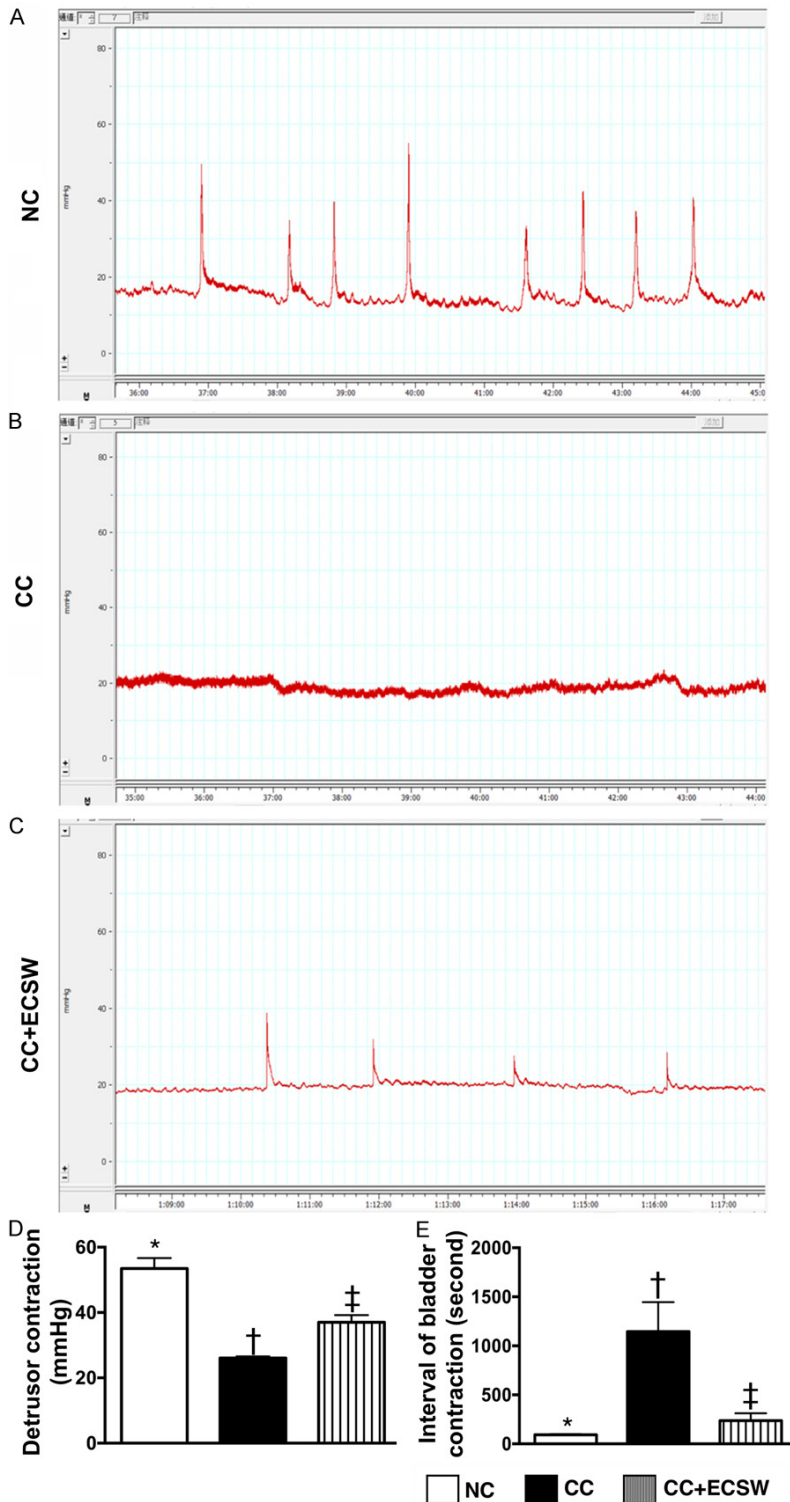


**Figure 1.** Pilot study, albuminuria and inflammatory biomarkers in urine, and urodynamic test of bladder contraction by day 28 after CC induction. Upper panel: (A, B) For determining the suitable dosage of radiation energy, we initially utilized 600 cGy/twice with four h interval for each animal in CC (A) and CC + ECSW (B) groups (n = 3/each group). By day 28 after CC induction, the results showed that no detrusor contractility wave to be observed in either CC only or

in CC + ECSW therapy animals. (C) Time courses of albumin concentration in 24-h urine: at day 1, \*vs. other groups with different symbols (†, ‡),  $P < 0.0001$ ; at day 7, \*vs. †,  $P < 0.001$ ; at day 14, \*vs. other groups with different symbols (†, ‡),  $P < 0.0001$ ; at day 28, \*vs. other groups with different symbols (†, ‡),  $P < 0.0001$ . (D) ELISA result of interleukin (IL)-6 level in 24-h urine by day 28 after CC induction, \*vs. other groups with different symbols (†, ‡),  $P < 0.001$ . (E) ELISA result of tumor necrosis factor (TNF)- $\alpha$  level in 24-h urine by day 28 after CC induction, \*vs. other groups with different symbols (†, ‡),  $P < 0.001$ . Lower panel: (A-C) Illustrating the urodynamic patterns of bladder contraction in NC (A), CC (B) and CC-ECSW (C), respectively. Significantly impaired detrusor contractility was identified in CC that was significantly reversed in animals with CC after receiving ECSW treatment. (D) Analytical result of detrusor contraction (mmHg) by day 28 after CC induction, \*vs. other groups with different symbols (†, ‡),  $P < 0.001$ . (E) Analytical result of mean time interval (second) of bladder contraction, \*vs. †,  $P < 0.001$ . All statistical analyses were performed by one-way ANOVA, followed by Bonferroni multiple comparison post hoc test (n = 6 for each group). Symbols (\*, †, ‡) indicate significance at the 0.05 level. NC = normal control; CC = chronic cystitis; ECSW = extracorporeal shock wave.

cystitis (CC) in the present study.

## Materials and methods

### Ethics and animal studies

All animal experimental protocols and procedures were approved by the institutional Animal Care and Use Committee at Kaohsiung Chang Gung Memorial

## ECSW against radiation-induced chronic cystitis

Hospital (Affidavit of Approval of Animal Use Protocol No. 2016012804) and executed in accordance with the Guide for the Care and Use of Laboratory Animals [The Eighth Edition of the Guide for the Care and Use of Laboratory Animals (NRC 2011)].

### *Animal model of chronic cystitis, animal grouping, and treatment*

Pathogen-free, adult male Sprague-Dawley (SD) rats (n = 24) weighing 325-350 g (Charles River Technology, BioLASCO Taiwan, Taiwan) were randomized and equally divided into normal control (NC) group, chronic cystitis (CC) group [induced by radiation to simulate brachytherapy (300 cGy twice) to the bladder surface over the skin at a time interval of 4 h], and CC + ECSW [(energy dosage of 0.2 mJ/mm<sup>2</sup>/120 impulses/at days 1, 7 and 14 after radiation exposure)]. ECSW was applied to the skin surface above the urinary bladder at different time points of treatment. During the procedures, all animals were anesthetized by inhalation of 2.0% isoflurane, and placed in a supine position on a warming pad at 37°C for radiation/ECSW.

### *The rationale of ECSW energy dosage and radiation dosage*

The ECSW energy chosen for the present study was based on our previous report [20] with some modifications. Initially, we utilized 600 cGy twice at four-hour interval for each animal in CC and CC + ECSW groups. However, urodynamic study by day 28 after CC induction showed no detrusor contraction activity in either CC only or in CC + ECSW therapy animals (**Figure 1A** and **1B**). On the other hand, when the radiotherapy dosage was reduced to 300 cGy twice at four-hour interval, detrusor contractility was significantly preserved after ECSW treatment (**Figure 2**). Accordingly, we modified the radiation energy to 300 cGy twice at four-hour interval for each animal in CC and CC + ECSW groups.

### *Collection of 24-hour urine for quantification of urine albumin, and sporadic urine for hematuria, urine protein, RBC/WBC counts at day 7, 14 and 28 after CC induction*

The procedure and protocol have been described in our previous reports [20, 29]. In details,

24-hour urine was collected in all animals at days 1, 7, 14 and 28 after CC induction to determine occulted blood, red blood cell count, white blood cell count, urine levels of albumin and protein and inflammation biomarkers.

For the collection of 24-hr urine for individual study, each animal was put in a metabolic cage [DXL-D, space: 190×290×550, Suzhou Fengshi Laboratory Animal Equipment Co. Ltd., Mainland China] for 24 hours with free access to food and water.

### *Immunohistochemical and immunofluorescent studies*

The procedures and protocols for immunohistochemistry (IHC) and immunofluorescence (IF) examinations were as previously described [20, 22, 24, 28-30]. In details, for IHC staining, rehydrated paraffin sections were first treated with 3% H<sub>2</sub>O<sub>2</sub> for 30 minutes and incubated with Immuno-Block reagent (BioSB) for 30 minutes at room temperature. Sections were then incubated with primary antibodies specifically against cytokeratin (CK)13, (1:400, Bioss, U.S.A.), CK17 (1:200, Abcam), CK18 (1:200, Abcam) and CK19 (1:200, Santa Cruz Biotechnology, U.S.A.) at 4°C overnight. Irrelevant antibodies and mouse control IgG were used as controls. IF staining was performed for the examination of CD14 (1:100, Santa Cruz Biotechnology, U.S.A.), CD68 (1:100 Abcam), COX-2 (1:100, Abcam), macrophage migration inhibitory factor (MIF) (1:100, Abcam) and substance P (1:500, Abcam) using appropriate primary antibodies; irrelevant antibodies were used as controls. Three sections of bladder specimens were analyzed in each rat.

For quantification, three randomly selected high-power fields (HPFs, 200× for IHC and IF studies) were analyzed in each section. The percentage of positively-stained cells per HPF for each animal was then determined. To analyze the integrity of collagen synthesis and deposition, three bladder paraffin sections (4 μm) were stained with picro-Sirius red (1% Sirius red in saturated picric acid solution) for one hour at room temperature using standard methods. The integrated area (μm<sup>2</sup>) of fibrosis in each section was calculated using Image Tool 3 (IT3) image analysis software (University of Texas, Health Science Center, San Antonio,

## ECSW against radiation-induced chronic cystitis

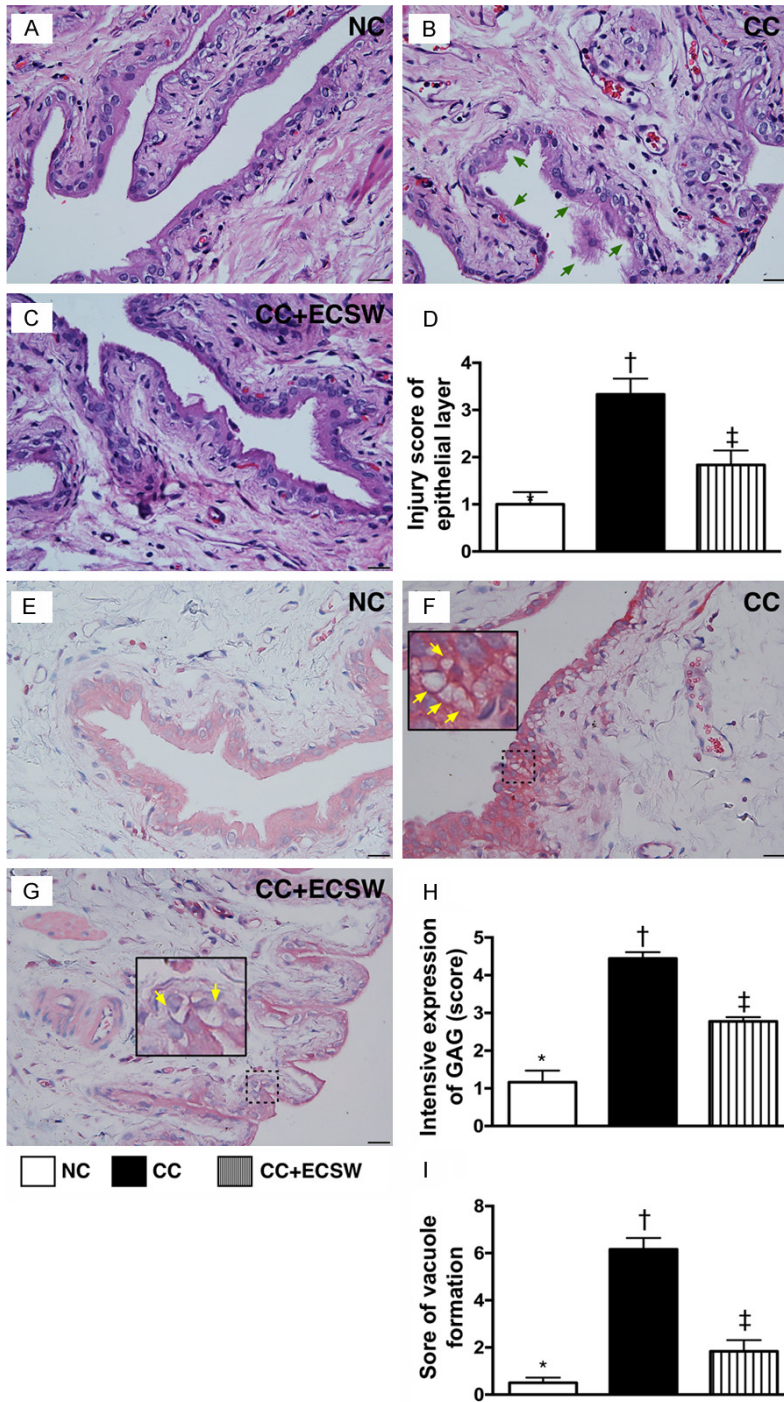


**Figure 2.** Histopathological findings of urinary bladder at day 28 after CC induction. (A-C) H and E stain (400 $\times$ ) for identification of injury of epithelial layer. The integrity of epithelial layer in CC was destroyed (B) (green arrows) as compared with NC (A) that was preserved in CC after receiving ECSW therapy (C). (D) Analytical result of the injury score of epithelial layer by day 28 after CC induction, \*vs. other groups with different symbols ( $\dagger$ ,  $\ddagger$ ),  $P < 0.0001$ . (E-G) immunohistochemical staining (400 $\times$ ) demonstrating intensive expression of glycosaminoglycan (GAG) in epithelial layer of urinary bladder (pink color). (H) Quantitative analysis of GAG expression, \*vs. other groups with different symbols ( $\dagger$ ,  $\ddagger$ ),  $P < 0.0001$ . (I) Quantification of vacuole formation (yellow arrows) in epithelial layer by day 28 after CC induction, solid square was the manifestation of dot-line square for identification of vacuole formation (yellow arrows), \*vs. other

groups with different symbols ( $\dagger$ ,  $\ddagger$ ),  $P < 0.0001$ . Scale bars in right lower corner represent 20  $\mu\text{m}$ . All statistical analyses were performed by one-way ANOVA, followed by Bonferroni multiple comparison post hoc test ( $n = 6$  for each group). Symbols (\*,  $\dagger$ ,  $\ddagger$ ) indicate significance at the 0.05 level. NC = normal control; CC = chronic cystitis; ECSW = extracorporeal shock wave.

UTHSCSA; Image Tool for Windows, Version 3.0, USA). Three selected sections were quantified for each animal. Three randomly selected HPFs (100 $\times$ ) were analyzed in each section. After determining the number of pixels in each fibrotic area per HPF, the numbers of pixels obtained from the three HPFs were summed. The procedure was repeated in two other sections for each animal. The mean pixel number per HPF for each animal was then determined by summing all pixel numbers and divided by 9. The mean integrated area ( $\mu\text{m}^2$ ) of fibrosis in quadriceps per HPF was obtained using a conversion factor of 19.24 (1  $\mu\text{m}^2$  corresponded to 19.24 pixels).

Histopathology scoring for the injury of epithelial layer in urinary bladder specimens from all animals was determined microscopically based on the results of Alcian Blue staining [i.e., for distributive intensity of glycosaminoglycan (GAG)] over the epithelial layer of urinary bladder was according to manufacturer's instruction. Additionally, h of 4  $\mu\text{m}$  sections. The grading of epithelial injury and

## ECSW against radiation-induced chronic cystitis

**Table 1.** Semi-quantitative results of sporadic urine-routine examinations at days 1, 7, 14 and 28 among the three groups

Variables	SC	CC	CC + ECSW	p-value*
Occulted blood	negative	negative	negative	-
Proteinuria	negative	negative	negative	-
Glucose	negative	negative	negative	-
Nitrate	positive	positive	positive	-
Red blood cell	0-1	0-1	0-1	-
White blood cell	0-1	6-10	0-1	<0.0001
Cast formation	none	none	none	-

Data are expressed as mean + SD. SC = sham control; CC = chronic cystitis; ECSW = extracorporeal shock wave. \*indicate n = 6 for each group per each time interval.

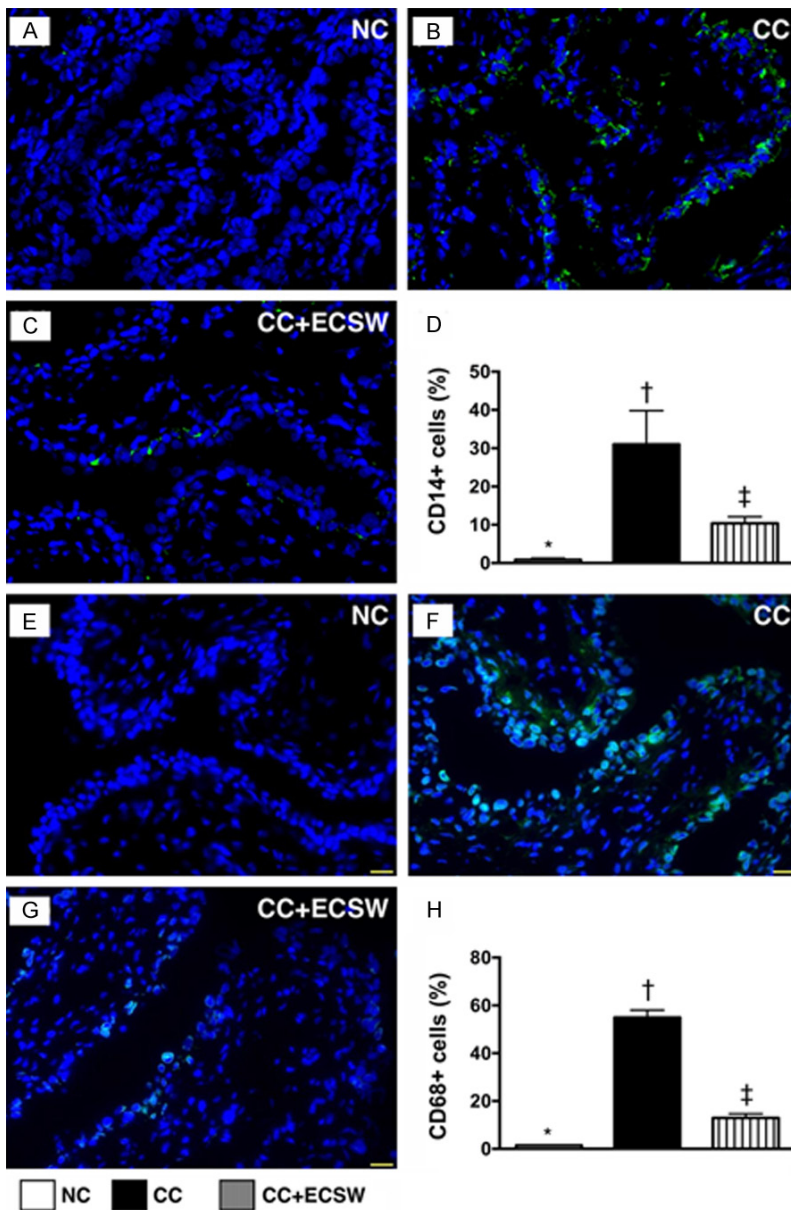


**Figure 3.** CD14+ and CD68+ cell expression in urinary bladder at day 28 after CC induction. A-C. Illustrating immunofluorescent (IF) microscopic find-

ing (400×) for identification of CD14+ cells (green color) in urinary bladder tissue by day 28 after CC induction. D. Analytical result of number of CD14+ cells by day 28 after CC induction, \*vs. other groups with different symbols (†, ‡),  $P < 0.0001$ . E-G. Illustrating IF microscopic finding (400×) for identification of CD68+ cells (green color) in urinary bladder tissue by day 28 after CC induction. H. Analytical result of number of CD68+ cells by day 28 after CC induction, \*vs. other groups with different symbols (†, ‡),  $P < 0.0001$ . All statistical analyses were performed by one-way ANOVA, followed by Bonferroni multiple comparison post hoc test (n = 6 for each group). Symbols (\*, †, ‡) indicate significance at the 0.05 level. NC = normal control; CC = chronic cystitis; ECSW = extracorporeal shock wave.

the formation of vacuoles (i.e., perinuclear cytoplasmic vacuolization) as well as for cytokeratin formation in the epithelial layer in 10 randomly chosen, non-overlapping fields (100×) for each animal was as follows: 0 (none), 1 ( $\leq 10\%$ ), 2 (11-25%), 3 (26-45%), 4 (46-75%), and 5 ( $\geq 76\%$ ).

### Western blot analysis

The procedure and protocol for Western blot analysis were based on our previous reports [20, 22, 24, 28-30]. Briefly, equal amounts (50  $\mu\text{g}$ ) of protein extracts were loaded and separated by SDS-PAGE using acrylamide gradients. After electrophoresis, the separated proteins were transferred electrophoretically to a polyvinylidene difluoride (PVDF) membrane (Amersham Biosciences). Nonspecific sites were blocked by incu-

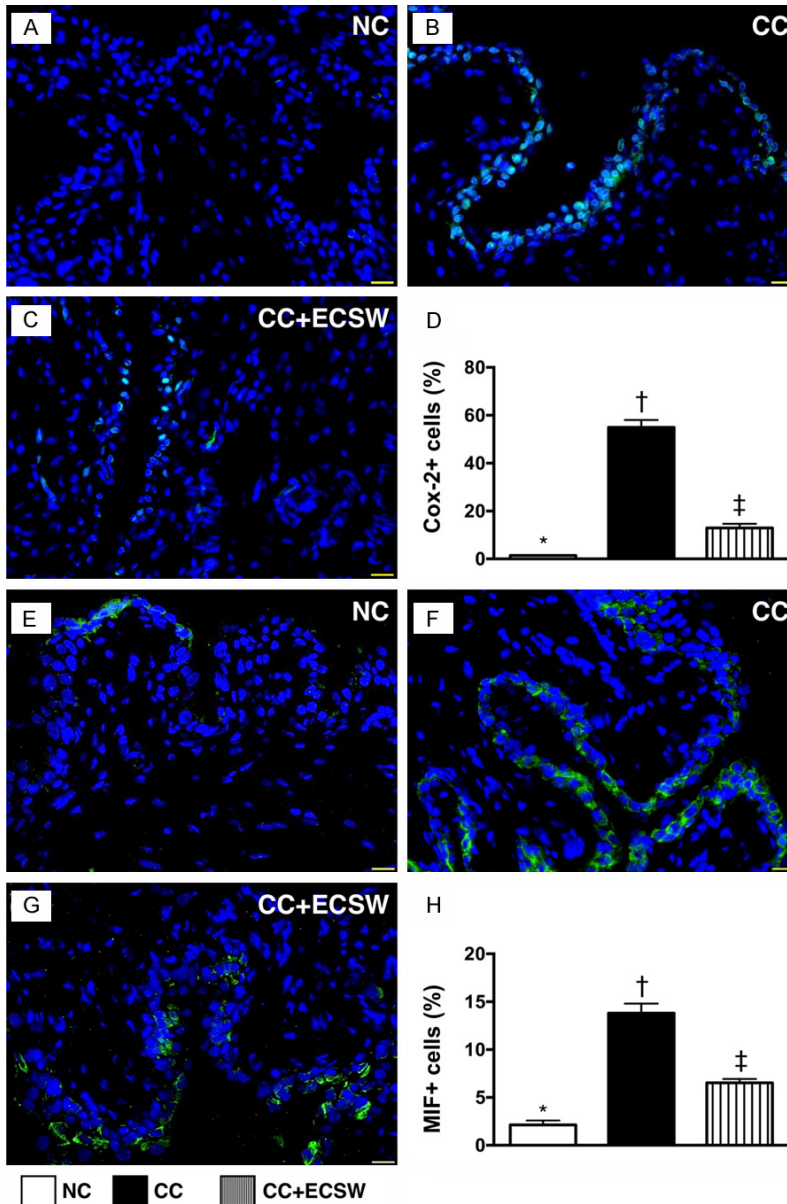


**Figure 4.** COX-2+ and MIF+ cell infiltration in urinary bladder at day 28 after CC induction. A-C. Illustrating immunofluorescent (IF) microscopic finding (400×) for identification of COX-2+ cells (green color) in urinary bladder by day 28 after CC induction. D. Analytical result of number of COX-2+ cells by day 28 after CC induction, \*vs. other groups with different symbols (†, ‡),  $P < 0.0001$ . E-G. Illustrating IF microscopic finding (400×) for identification of macrophage migration inhibitor factor (MIF)+ cells (green color) in urinary bladder by day 28 after CC induction. H. Analytical result of number of MIF+ cells by day 28 after CC induction, \*vs. other groups with different symbols (†, ‡),  $P < 0.0001$ . All statistical analyses were performed by one-way ANOVA, followed by Bonferroni multiple comparison post hoc test ( $n = 6$  for each group). Symbols (\*, †, ‡) indicate significance at the 0.05 level. NC = normal control; CC = chronic cystitis; ECSW = extracorporeal shock wave.

ies [matrix metalloproteinase (MMP)-9 (1:1000, Abcam), tumor necrosis factor (TNF)- $\alpha$  (1:1000, Cell Signaling), nuclear factor (NF)- $\kappa$ B (1:600, Abcam), NOX-1 (1:1500, Sigma), NOX-2 (1:750, Sigma), interleukin (IL)-6 (1:1000, Abcam), IL-12 (1:1000, Abcam), RANTES (1:1000, Cell Signaling), inducible nitric oxide synthase (iNOS) (1:1000, Abcam), toll-like receptor (TLR)-2 (1:1000, Abcam), TLR-4 (1:1000, Abcam), mitochondrial Bax (1:1000, Abcam), cleaved caspase 3 (1:1000, Cell Signaling), cleaved poly (ADP-ribose) polymerase (c-PARP) (1:1000, Cell Signaling), transforming growth factor (TGF)- $\beta$  (1:500, Abcam), phosphorylated (p)-Smad3 (1:1000, Cell Signaling), p-Smad1/5 (1:1000, Cell Signaling), bone morphogenetic protein (BMP)-2 (1:500, Abcam) and actin (1:10000, Chemicon)] for 1 hour at room temperature. Horseradish peroxidase-conjugated anti-rabbit immunoglobulin IgG (1:2000, Cell Signaling) was used as a secondary antibody for one-hour incubation at room temperature. Immunoreactive bands were visualized by enhanced chemiluminescence (ECL; Amersham Biosciences) and exposed to Biomax L film (Kodak). For the purpose of quantification, ECL signals were digitized using Labwork software (UVP).

#### Assessment of oxidative stress

bation of the membrane in blocking buffer [5% nonfat dry milk in T-TBS (TBS containing 0.05% Tween 20)] overnight. The membranes were incubated with the indicated primary antibod-

The procedure and protocol for assessing the protein expression of oxidative stress have been described in details in our previous reports [20, 22, 24, 28-30]. The Oxyblot

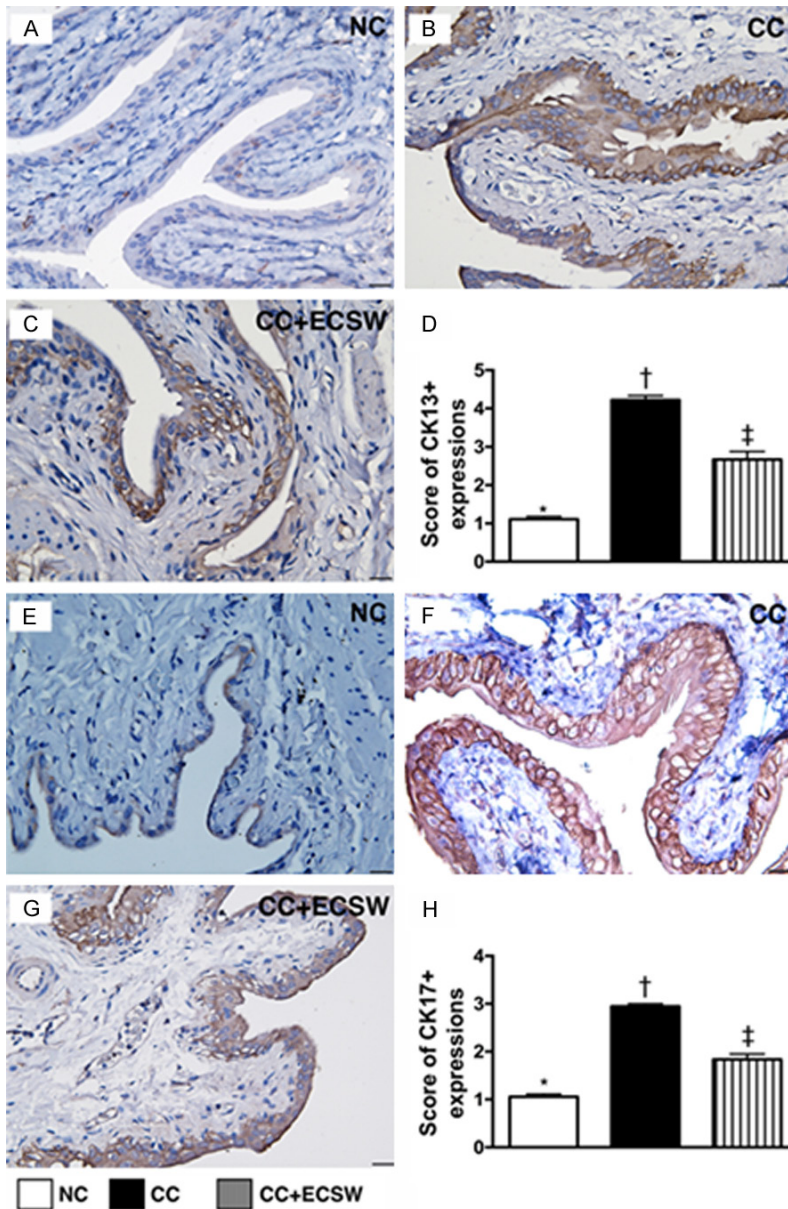


**Figure 5.** Expressions of cytokeratin (CK)13+ and CK17+ cells in urinary bladder at day 28 after CC induction. A-C. Illustrating microscopic finding (400×) of immunohistochemical (IHC) staining for assessing the expression of CK13+ cells infiltrated in bladder (brown color) in urinary bladder by day 28 after CC induction. D. Analytical results of number of CK13+ cells by day 28 after CC induction, \*vs. other groups with different symbols (†, ‡),  $P < 0.0001$ . E-G. Microscopic finding (400×) of IHC staining for identification of the expression of CK17+ cells infiltrated in bladder (brown color) in urinary bladder by day 28 after CC induction. H. Analytical results of number of CK17+ cells by day 28 after CC induction, \*vs. other groups with different symbols (†, ‡),  $P < 0.0001$ . Scale bars in right lower corner represent 20  $\mu\text{m}$ . All statistical analyses were performed by one-way ANOVA, followed by Bonferroni multiple comparison post hoc test ( $n = 6$  for each group). Symbols (\*, †, ‡) indicate significance at the 0.05 level. NC = normal control; CC = chronic cystitis; ECSW = extracorporeal shock wave.

was carried out on 6  $\mu\text{g}$  of protein for 15 minutes according to the manufacturer's instructions. One-dimensional electrophoresis was carried out on 12% SDS/polyacrylamide gel after DNPH derivatization. Immunoreactive bands were visualized by enhanced chemiluminescence (ECL; Amersham Biosciences) which was then exposed to Biomax L film (Kodak). For quantification, ECL signals were digitized using Labwork software (UVP). For oxyblot protein analysis, a standard control was loaded on each gel.

*Procedure and protocol of urodynamic test (bladder pressure assessment)*

The procedure of intravesical pressure measurement was in accordance with that previously reported [31]. After being anesthetized with 2.0% inhalational isoflurane, the rat was placed in supine position on a heating pad maintained at 37°C. A polyethylene catheter (PE50, Clay Adams, NJ, USA), which was inserted through the urethra into the urinary bladder, was connected to a pressure transducer (BP Transducer Model MLT03-80, Ad Instruments, Bella Vista, NSW, Australia) and syringe pump (Microinjection pump Model KDS100, KD Scientific Inc. 84 October Hill Road Holliston, MA 01756 USA) that delivered normal saline to the urinary bladder at a rate of 0.05 mL/min. Intravesical pressure analog signals, which were recorded continuously for 90 minutes, were converted real-

Oxidized Protein Detection Kit was purchased from Chemicon (S7150). DNPH derivatization

pressure analog signals, which were recorded continuously for 90 minutes, were converted real-



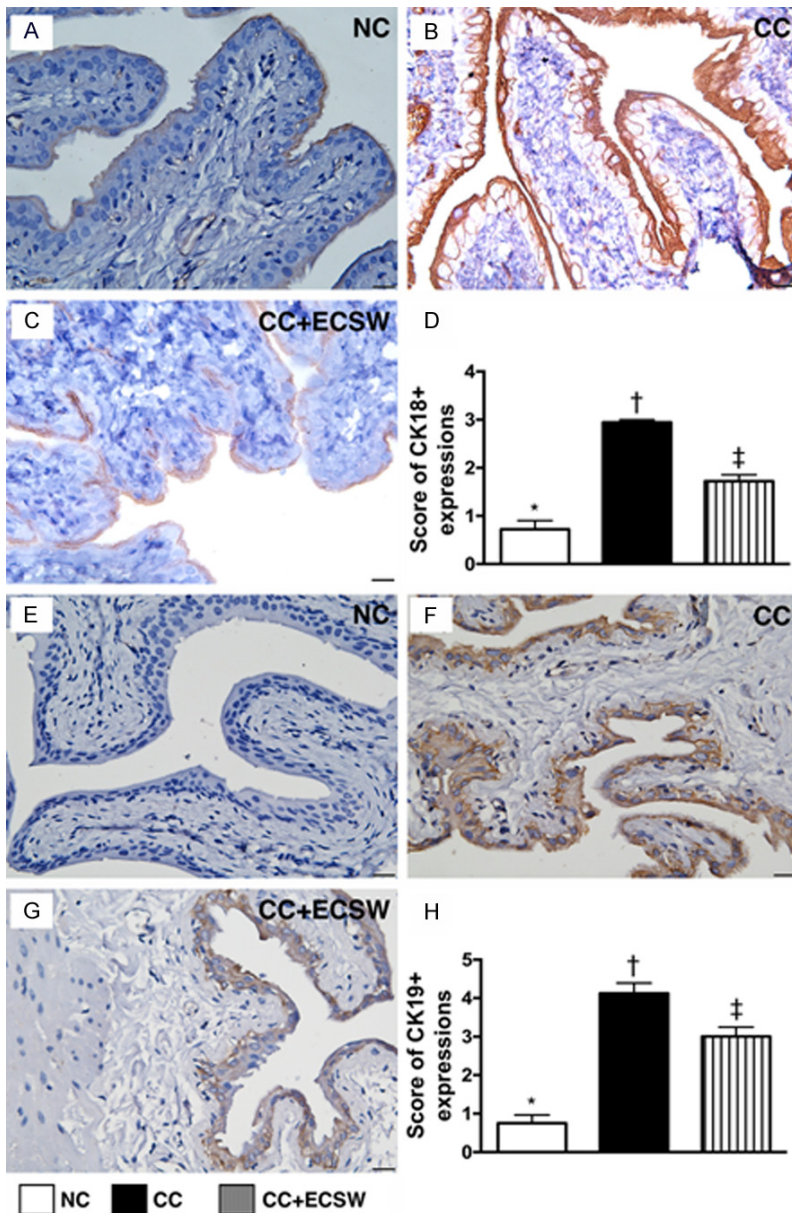


**Figure 6.** Expressions of cytokeratin (CK)18+ and CK19+ cells in urinary bladder at day 28 after CC induction. A-C. Illustrating microscopic finding (400×) of immunohistochemical (IHC) staining for assessing the expression of CK18+ cells infiltrated in bladder (brown color) in urinary bladder by day 28 after CC induction. D. Analytical results of number of CK18+ cells by day 28 after CC induction, \*vs. other groups with different symbols (†, ‡),  $P < 0.0001$ . E-G. Microscopic finding (400×) of IHC staining for identification of the expression of CK19+ cells infiltrated in bladder (brown color) in urinary bladder by day 28 after CC induction. H. Analytical results of number of CK19+ cells by day 28 after CC induction, \*vs. other groups with different symbols (†, ‡),  $P < 0.0001$ . Scale bars in right lower corner represent 20  $\mu\text{m}$ . All statistical analyses were performed by one-way ANOVA, followed by Bonferroni multiple comparison post hoc test ( $n = 6$  for each group). Symbols (\*, †, ‡) indicate significance at the 0.05 level. NC = normal control; CC = chronic cystitis; ECSW = extracorporeal shock wave.

NSW, Australia) and amplified (Bridge Amp Model FE221, and Animal Bio Amp Model: FE136, Ad Instruments, Bella Vista, NSW, Australia) before being stored in a computer for later analysis (PowerLab 16/35 Model PL35-16, Ad Instruments, Bella Vista, NSW, Australia).

*Statistical analysis*

Quantitative data are expressed as means  $\pm$  SD. Statistical analysis was adequately performed by ANOVA followed by Bonferroni multiple-comparison post hoc test. SAS statistical software for Windows version 8.2 (SAS institute, Cary, NC) was utilized. A probability value  $< 0.05$  was considered statistically significant.

**Results**

*Pilot study of 600 cGy/ twice with four h interval for assessment the severity of detrusor functional impairment and urodynamic study of bladder contraction at day-28 after radiotherapy (Figure 1)*

The results ( $n = 3$  in each group) demonstrated that no any contractile signaling was identified in either CC group or CC + ECSW group at the day 28 after radiotherapy (Upper panel: **Figure 1A, 1B**), suggesting that the radiotherapy with 600 cGy/twice with four h interval was too much high that was not suitable for our study purpose, therefore, the modified dosage

of radiotherapy was conducted in the present study.

time into electrical signals (PowerLab 16/35 Model PL3516, Ad Instruments, Bella Vista,

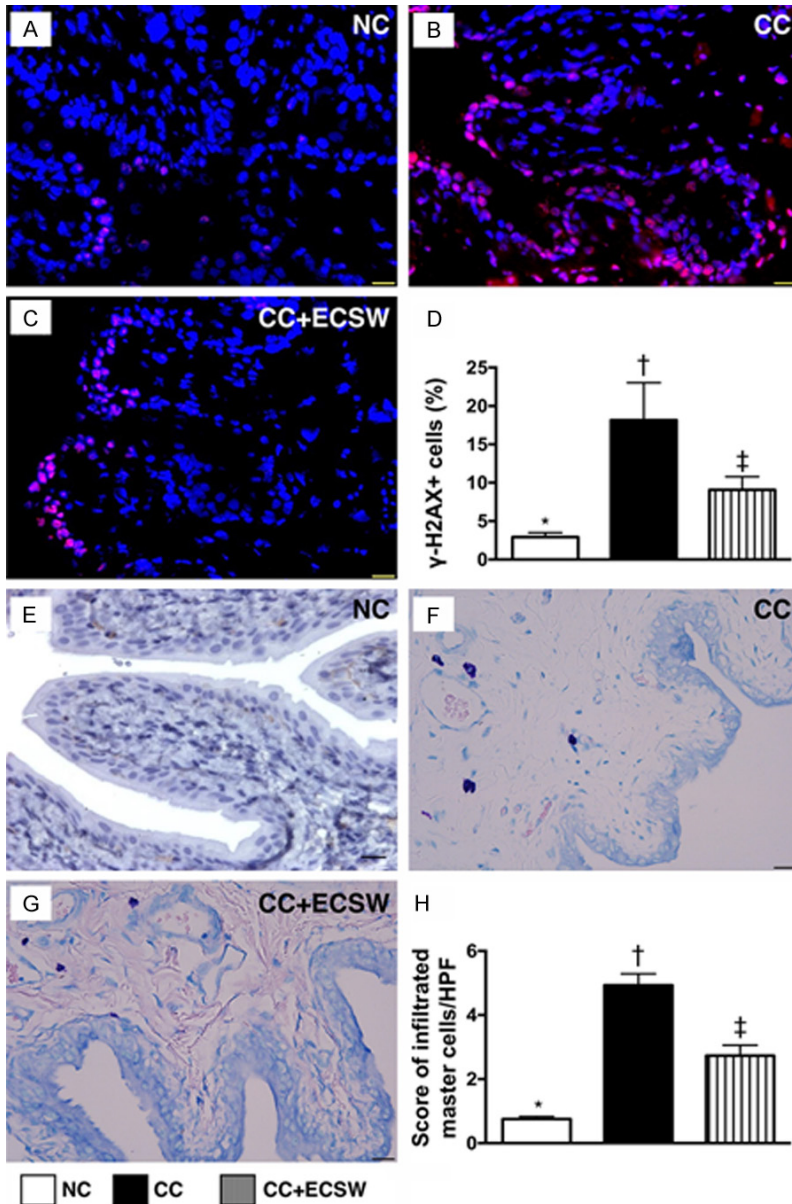


**Figure 7.** Cellular expressions of DNA-damaged and inflammatory biomarkers in urinary bladder at day 28 after CC induction. A-C. Illustrating microscopic finding (400×) of immunofluorescent staining for assessing the expression of  $\gamma$ -H2AX+ cells infiltrated in bladder (pink color) in urinary bladder by day 28 after CC induction. D. Analytical results of number of  $\gamma$ -H2AX+ cells by day 28 after CC induction, \*vs. other groups with different symbols (†, ‡),  $P < 0.0001$ . E-G. Microscopic finding (400×) of Giemsa staining for identification of the expression of mast cells infiltrated in bladder (deep-blue color) by day 28 after CC induction. H. Analytical results of number of mast cells by day 28 after CC induction, \*vs. other groups with different symbols (†, ‡),  $P < 0.0001$ . Scale bars in right lower corner represent 20  $\mu$ m. All statistical analyses were performed by one-way ANOVA, followed by Bonferroni multiple comparison post hoc test ( $n = 6$  for each group). Symbols (\*, †, ‡) indicate significance at the 0.05 level. NC = normal control; CC = chronic cystitis; ECSW = extracorporeal shock wave.

The urodynamic patterns showed that as compared with NC, significantly impaired detrusor contractility was identified in CC that was significantly reversed in animals with CC after

receiving ECSW treatment (Lower panel: **Figure 1A-E**).

*Time courses of sporadic urine-routine examination and 24-h urine for determining the proinflammatory biomarkers and albumin level at the end of study period (Table 1 and upper panel of Figure 1)*

Urine routine results showed that the occulted blood, proteinuria, glucose, nitrate, red blood cell count and cast formation in sporadic urine sample were found to be within the normal range at the time points of days 1, 7, 14 and 28 (Table 1). However, the white blood cell count in these time points were significantly higher in CC than in normal control (NC) and CC-ECSW but it showed no difference between the later two groups (Table 1).

On the other hand, the albumin concentration in 24-h urine was significantly higher in CC-ECSW than in NC and CC, but it showed no difference between NC and CC at day 1, significantly higher in CC and CC-ECSW than in NC, but it showed no difference between CC and CC-ECSW at day 7, significantly higher in CC than in NC and CC-ECSW and significantly higher in CC-ECSW than in NC at days 14 and 28 after radiotherapy (Upper panel: **Figure 1C**). These findings suggest that ECSW temporally increased urinary bladder permeability, and radio-

therapy damaged the mucosa of urinary bladder, resulted in progressively increased the leakage of albumin from the urinary bladder into the urine.

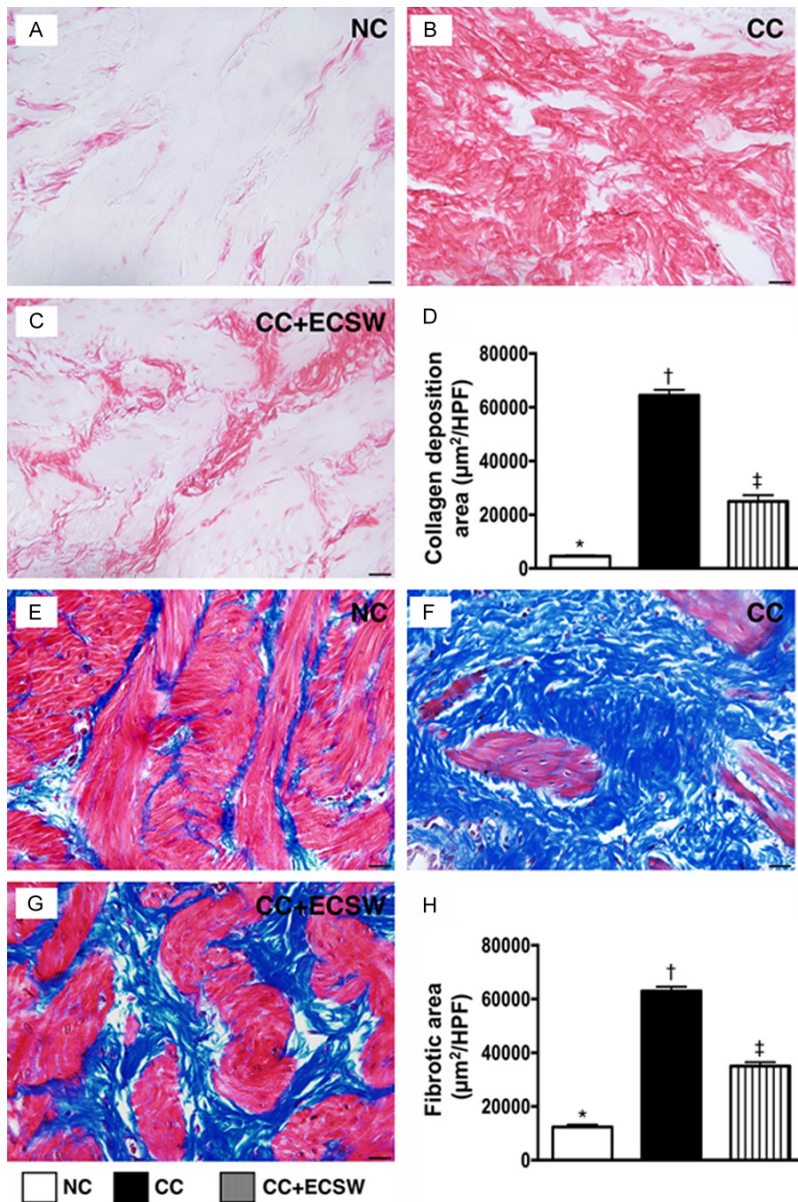


**Figure 8.** Condensed collagen-deposition and fibrotic areas in urinary bladder at day 28 after CC induction. A-C. Illustrating the microscopic finding (400×) of Sirius stain for identification of condensed collagen-deposition area in urinary bladder (pink color) in urinary bladder by day 28 after CC induction. D. Analytical result of microscopic finding by day 28 after CC induction, \*vs. other groups with different symbols (†, ‡),  $P < 0.0001$ . E-G. Showing the microscopic finding (400×) of Masson's trichrome stain for identification of fibrotic area in urinary bladder (blue color) in urinary bladder by day 28 after CC induction. H. Analytical result of microscopic finding by day 28 after CC induction, \*vs. other groups with different symbols (†, ‡),  $P < 0.0001$ . Scale bars in right lower corner represent 20 µm. All statistical analyses were performed by one-way ANOVA, followed by Bonferroni multiple comparison post hoc test ( $n = 6$  for each group). Symbols (\*, †, ‡) indicate significance at the 0.05 level. NC = normal control; CC = chronic cystitis; ECSW = extracorporeal shock wave.

Furthermore, by day 28 after radiotherapy, the enzyme-linked immunosorbent assay (ELISA) results showed that the urine levels of interleu-

kin (IL)-6 and tumor necrosis factor (TNF)- $\alpha$ , two indicators of inflammation, were significantly higher in CC than in NC and CC-ECSW and significantly higher in CC-ECSW than in NC (Upper panel: **Figure 1D, 1E**).

*Histopathological findings of urinary bladder at day 28 after CC induction (Figure 2)*

The H&E stain demonstrated that the injury score of epithelial layer was significantly increased in the CC group than that in NC group and in the CC-ECSW group, and significantly increased in the CC-ECSW group than that in NC group. In addition, IHC staining showed that the expression of GAG in the epithelial layer of the bladder, an indicator of disruption of the bladder mucosa surface layer, displayed an identical pattern compared to that of c injury score of epithelial layer among the three groups. Furthermore, the formation of vacuoles in epithelial layer also showed a pattern identical to that of injury score of epithelial layer among the three groups.

*Inflammatory cell infiltration in urinary bladder at day 28 after CC induction (Figures 3 and 4)*

IHC staining demonstrated that the numbers of CD68+ and CD14+ cells (**Figure 3**), two cellular biomarkers of inflammation, were significantly higher in the untreated CC group than that in the NC and in the CC-ECSW group, and significantly higher in the CC-ECSW animals than that in NC. Consistently, IF staining demonstrated

## ECSW against radiation-induced chronic cystitis

that the expressions of macrophage migration inhibitory factor (MIF)+ and cyclooxygenase (COX)-2+ (**Figure 4**) cells in the bladder, another two typical markers of acute inflammatory cells, were similar to those of CD68+ and CD14+ cells in the urinary bladder among the three groups.

*Expressions of cytokeratin (CK)13+, CK+17, CK+18 and CK+19 cells and collagen-deposition/fibrotic area in urinary bladder at day 28 after CC Induction (Figures 5-8)*

IHC staining showed that the expressions of CK13+ (**Figure 5**) and CK17+ cell (**Figure 5**), two indicators of keratin-phenotype epithelial cells, were significantly higher in the untreated CC animals than those in the NC and in the CC-ECSW group, and significantly higher in the CC-ECSW group than those in the NC.

Additionally, IHC staining revealed that the pattern of expressions of CK18+ (**Figure 6**), and CK19+ (**Figure 6**) cells, another two indicators of keratin-phenotype epithelial cells, were identical to that of the expression of CK13+ cells among the three groups. Furthermore, the cellular expression of  $\gamma$ -H2AX (**Figure 7**), an indicator of DNA damage and mast cell (**Figure 7**), an indicator of inflammation, showed an identical pattern compared to that of CK13+ cells among the three groups. Moreover, Masson's trichrome staining showed that the fibrotic area (**Figure 8**) and Sirius stain showed that the condensed collagen-deposition area (**Figure 8**) exhibited an identical pattern compared to that of  $\gamma$ -H2AX+ cells among all groups.

*Protein expressions of inflammatory biomarkers at day 28 after CC induction (Figure 9)*

The protein expressions of IL-6, IL-12, matrix metalloproteinase (MMP)-9, TNF- $\alpha$ , nuclear factor (NF)- $\kappa$ B, RANTES and inducible nitric oxide synthase (iNOS), seven indicators of inflammation, were significantly higher in the CC group than those in NC and in the CC-ECSW group, and significantly higher in the CC-ECSW group than those in the NC.

*Protein expressions of oxidative stress, toll-like receptor (TLR), apoptotic, fibrotic and anti-apoptotic biomarkers at day 28 after CC Induction (Figure 10)*

The protein expressions of NOX-1, NOX-2 and oxidized protein, three indices of oxidative stress, were significantly higher in the untreated CC animals than those in NC and in the

CC-ECSW group, and significantly higher in the CC-ECSW group than those in NC. Additionally, TLR-2 and TLR-4, two indicators of innate inflammatory reaction displayed an identical pattern to those of oxidative stress among the three groups.

The protein expression of mitochondrial Bax, cleaved caspase 3 and cleaved PARP, three indices of apoptosis, were significantly higher in the untreated CC animals than those in NC and in the CC-ECSW group, and significantly higher in the CC-ECSW group than those in NC. Additionally, protein expression of TGF- $\beta$  and Smad3, two indicators of fibrosis, exhibited an identical pattern of apoptosis whereas the Smad1/5 and BMP-2) two indicators of anti-fibrosis, displayed an opposite pattern of apoptosis among the three groups. The proposed mechanisms for positive therapeutic effects of ECSW on preserving of bladder function from radiotherapy-induced chronic cystitis and the raw materials of Western blot ([Supplementary Figures 1 and 2](#)).

### Discussion

Previous clinical observation studies have shown that radiotherapy frequently induce gross hematuria and hemorrhagic cystitis as well as CC which not only limited the patient's quality of life, but also induce obstructive uropathy and renal failure, resulted in an increase the risk of morbidity and mortality [2-7]. One important finding in the present study is that, as compared with the control animals, detrusor contractility (i.e., functional integrity of urinary bladder) was substantially impaired, whereas albuminuria was remarkably aggravated in untreated CC animals, suggesting the successful creation of a useful animal model not only for the present study but also for future investigation. Our experimental findings were consistent with those of previous observational studies [2-7].

The treatment of chemotherapy/radiotherapy-induced hemorrhagic cystitis and CC remain a formidable challenge because many of the reported therapeutic strategies [8-19] are still partially effective with unacceptably high failure rates. The most important finding in the present study is that impaired detrusor function and albuminuria were notably improved in CC animals after ECSW treatment. Our findings, in addition to extending those of previous studies [8-19], raise the need for a possible prospective clinical trial to evaluate the therapeutic

## ECSW against radiation-induced chronic cystitis

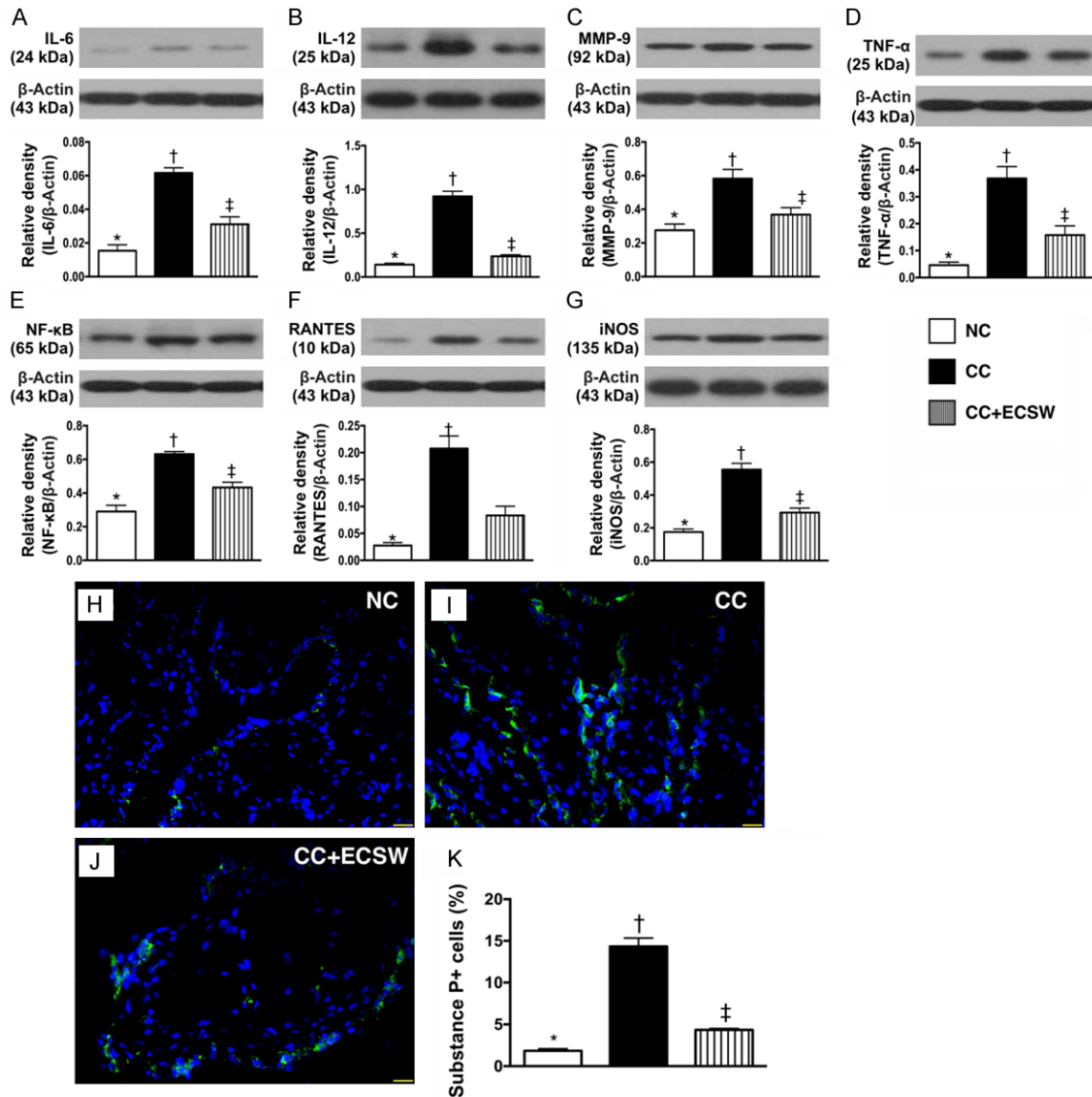
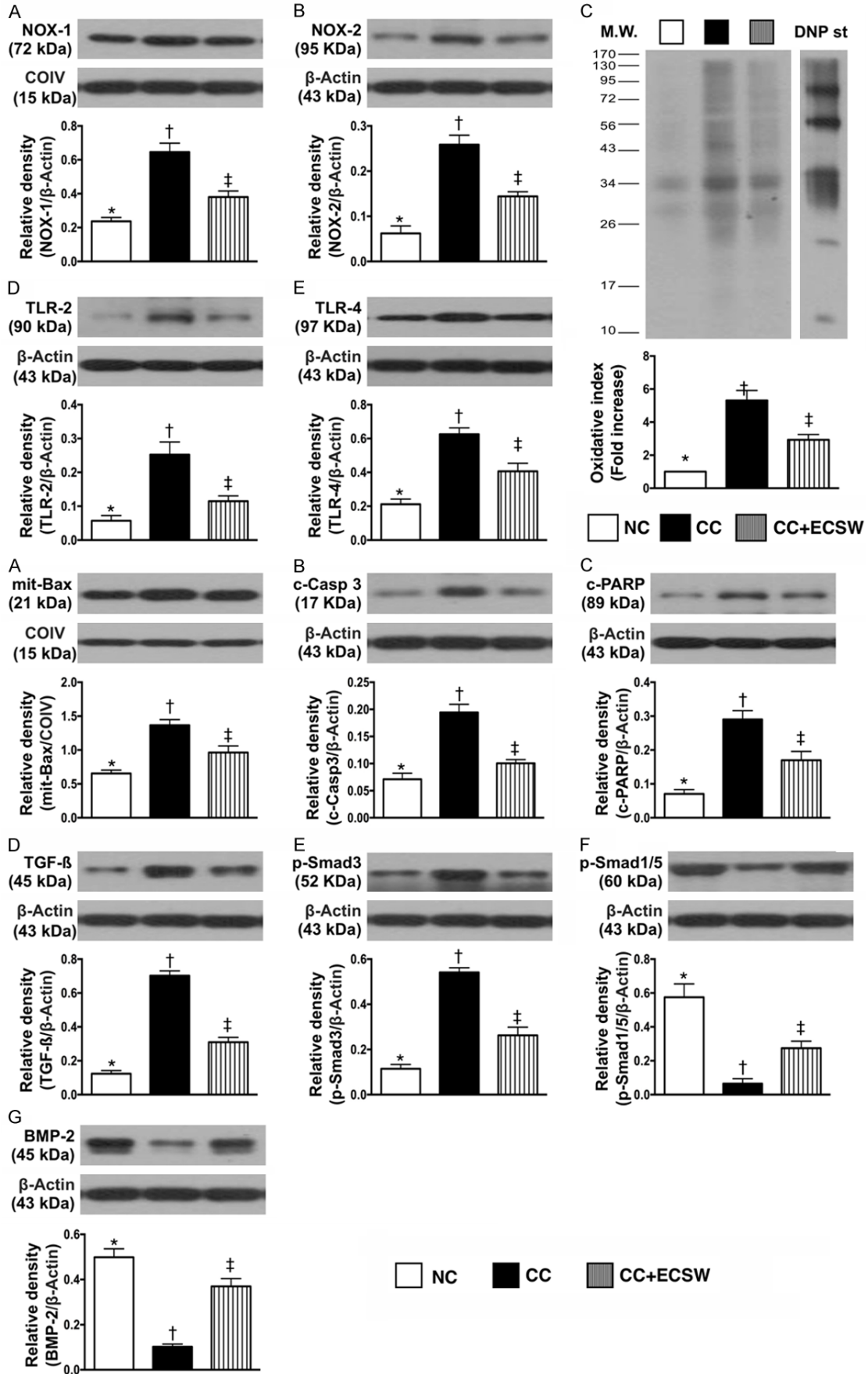


**Figure 9.** Protein and cellular expressions of inflammatory biomarkers in urinary bladder at day 28 after CC induction. A. Protein expression of interleukin (IL)-6 in urinary bladder by day 28 after CC induction, \*vs. other groups with different symbols (†, ‡),  $P < 0.001$ . B. Protein expression of IL-12 in urinary bladder by day 28 after CC induction, \*vs. other groups with different symbols (†, ‡),  $P < 0.001$ . C. Protein expression of matrix metalloproteinase (MMP)-9 in urinary bladder by day 28 after CC induction, \*vs. other groups with different symbols (†, ‡),  $P < 0.001$ . D. Protein expression of tumor necrosis factor (TNF)- $\alpha$  in urinary bladder by day 28 after CC induction, \*vs. other groups with different symbols (†, ‡),  $P < 0.001$ . E. Protein expression of nuclear factor (NF)- $\kappa$ B in urinary bladder by day 28 after CC induction, \*vs. other groups with different symbols (†, ‡),  $P < 0.001$ . F. Protein expression of RANTES in urinary bladder by day 28 after CC induction, \*vs. other groups with different symbols (†, ‡),  $P < 0.0001$ . G. Protein expression of inducible nitric oxide synthase (iNOS) in urinary bladder by day 28 after CC induction, \*vs. other groups with different symbols (†, ‡),  $P < 0.001$ . H-J. Illustrating IF microscopic finding (400x) for identification of substance P (SP)+ cells (green color) in urinary bladder by day 28 after CC induction. K. Analytical result of number of substance P+ cells by day 28 after CC induction, \*vs. other groups with different symbols (†, ‡),  $P < 0.0001$ . Scale bars in right lower corner represent 20  $\mu$ m. All statistical analyses were performed by one-way ANOVA, followed by Bonferroni multiple comparison post hoc test ( $n = 6$  for each group). Symbols (\*, †, ‡) indicate significance at the 0.05 level. NC = normal control; CC = chronic cystitis; ECSW = extracorporeal shock wave.

tic potential of ECSW in patients experiencing hemorrhagic cystitis and CC refractory to conventional therapy.

Associations among increase in inflammatory reaction, generation of oxidative stress, and tissue/organ damage have been keenly investi-

# ECSW against radiation-induced chronic cystitis



## ECSW against radiation-induced chronic cystitis

**Figure 10.** Protein expressions of oxidative stress, toll-like receptor and apoptotic, fibrotic and anti-apoptotic biomarkers in urinary bladder at day 28 after CC Induction. Upper panel: A. Protein expression of NOX-1 in urinary bladder by day 28 after CC induction, \*vs. other groups with different symbols (†, ‡),  $P < 0.0001$ . B. Protein expression of NOX-2 in urinary bladder by day 28 after CC induction, \*vs. other groups with different symbols (†, ‡),  $P < 0.001$ . C. Oxidized protein expression in urinary bladder by day 28 after CC induction, \* vs. other groups with different symbols (†, ‡),  $P < 0.001$ . (Note: left and right lanes shown on the upper panel represent protein molecular weight marker and control oxidized molecular protein standard, respectively). M.W = molecular weight; DNP = 1-3 dinitrophenylhydrazine. D. Protein expression of toll-like receptor (TLR)-2 in urinary bladder by day 28 after CC induction, \*vs. other groups with different symbols (†, ‡),  $P < 0.001$ . E. Protein expression of TLR-4 in urinary bladder by day 28 after CC induction, \* vs. other groups with different symbols (†, ‡),  $P < 0.001$ . All statistical analyses were performed by one-way ANOVA, followed by Bonferroni multiple comparison post hoc test ( $n = 6$  for each group). Symbols (\*, †, ‡) indicate significance at the 0.05 level. NC = normal control; CC = chronic cystitis; ECSW = extracorporeal shock wave. Lower panel: A. Protein expression of mitochondrial Bax (mit-Bax) in urinary bladder by day 28 after CC induction, \*vs. other groups with different symbols (†, ‡),  $P < 0.001$ . B. Protein expression of cleaved caspase 3 (c-Casp 3) in urinary bladder by day 28 after CC induction, \*vs. other groups with different symbols (†, ‡),  $P < 0.001$ . C. Protein expression of cleaved poly (ADP-ribose) polymerase (c-PARP) in urinary bladder by day 28 after CC induction, \*vs. other groups with different symbols (†, ‡),  $P < 0.001$ . D. Protein expression of transforming growth factor (TGF)- $\beta$  in urinary bladder by day 28 after CC induction, \* vs. other groups with different symbols (†, ‡, §),  $P < 0.001$ . E. Protein expression of phosphorylated (p)-Smad3 in urinary bladder by day 28 after CC induction, \*vs. other groups with different symbols (†, ‡),  $P < 0.001$ . F. Protein expression of p-Smad1/5 in urinary bladder by day 28 after CC induction, \*vs. other groups with different symbols (†, ‡),  $P < 0.001$ . G. Protein expression of bone morphogenesis protein (BMP)-2 in urinary bladder by day 28 after CC induction, \*vs. other groups with different symbols (†, ‡),  $P < 0.001$ . All statistical analyses were performed by one-way ANOVA, followed by Bonferroni multiple comparison post hoc test ( $n = 6$  for each group). Symbols (\*, †, ‡) indicate significance at the 0.05 level. NC = normal control; CC = chronic cystitis; ECSW = extracorporeal shock wave.

gated in previous studies [14, 20-22, 25, 27]. An essential finding in the present study is that inflammatory reactions (i.e., in tissue and urine level) were significantly enhanced in the untreated CC group compared to those in the NC at both cellular and molecular levels. Moreover, the generation of oxidative stress as well as the expressions of DNA and mitochondrial damage markers were remarkably upregulated in the CC group as compared with those in the NC. At histological level, the integrity of epithelial layer and architecture of smooth muscle layer were markedly destroyed and keratin-phenotype epithelial cells were substantially increased in untreated CC animals compared with that in the NC. Our findings, therefore, corroborated those of previous studies [14, 20-22, 25, 27].

Interestingly, our previous study has also shown that ECSW treatment significantly protected against cyclophosphamide-induced acute interstitial cystitis in rats [20]. The principal finding in the present study is that these molecular-cellular perturbations were markedly attenuated and the architectural integrity of urinary bladder was notably preserved in CC animals after ECSW treatment. In this way, our findings, in addition to strengthening those of our previous study [20], highlight the potential clinical application of ECSW in patients with hemorrhagic cystitis and CC refractory to conventional treatment strategies.

The mechanisms underlying the therapeutic effects of ECSW against various diseases that have been extensively investigated, including (1) removal of free radicals and acting as an anti-oxidant, (2) suppression of oxidative stress and inflammation as well as upregulation of endogenous nitric oxide production, (3) enhancement of angiogenesis, and (4) pain-alleviation [20, 22-28]. In the present study, although extensive work has been done to elucidate the therapeutic effect of ECSW in the setting of radiation-induced CC, the exact underlying mechanisms remain unclear. The proposed mechanisms underlying the observed protective effects of Mel-Ex4 treatment against radiation-induced chronic cystitis based on our findings have been summarized in [Supplementary Figure 1](#).

### *Study limitations*

This study has limitations. First, the study period of merely 28 days was not enough for long-term follow-up to determine whether hematuria (i.e., hemorrhagic cystitis) was present in both untreated and ECSW-treated CC rats. Second, without comparison with other therapeutic agents, it remains unclear whether ECSW treatment is superior to conventional medications or vice versa.

In conclusion, ECSW treatment markedly attenuated radiation-induced CC in a rodent model,

including alleviation of hematuria and proteinuria as well as preservation of histological integrity of the urinary bladder, through suppression of inflammation, oxidative stress, and epithelial damage.

### Acknowledgements

This study was supported by a program grant from Chang Gung Memorial Hospital, Chang Gung University (Grant number: CRRPG8F0481 and CRRPG8F0482).

### Disclosure of conflict of interest

None.

**Address correspondence to:** Dr. Hon-Kan Yip, Division of Cardiology, Department of Internal Medicine, Kaohsiung Chang Gung Memorial Hospital and Chang Gung University College of Medicine, Kaohsiung 83301, Taiwan. Tel: +886-7-7317123; Fax: +886-7-7322402; E-mail: han.gung@msa.hinet.net; Dr. Cheuk-Kwan Sun, Department of Emergency Medicine, E-Da Hospital, I-Shou University School of Medicine for International Students, Kaohsiung 82445, Taiwan. Tel: +886-7-6150011 Ext. 1007; Fax: +886-7-7322402; E-mail: lawrence.c.k.sun@gmail.com

### References

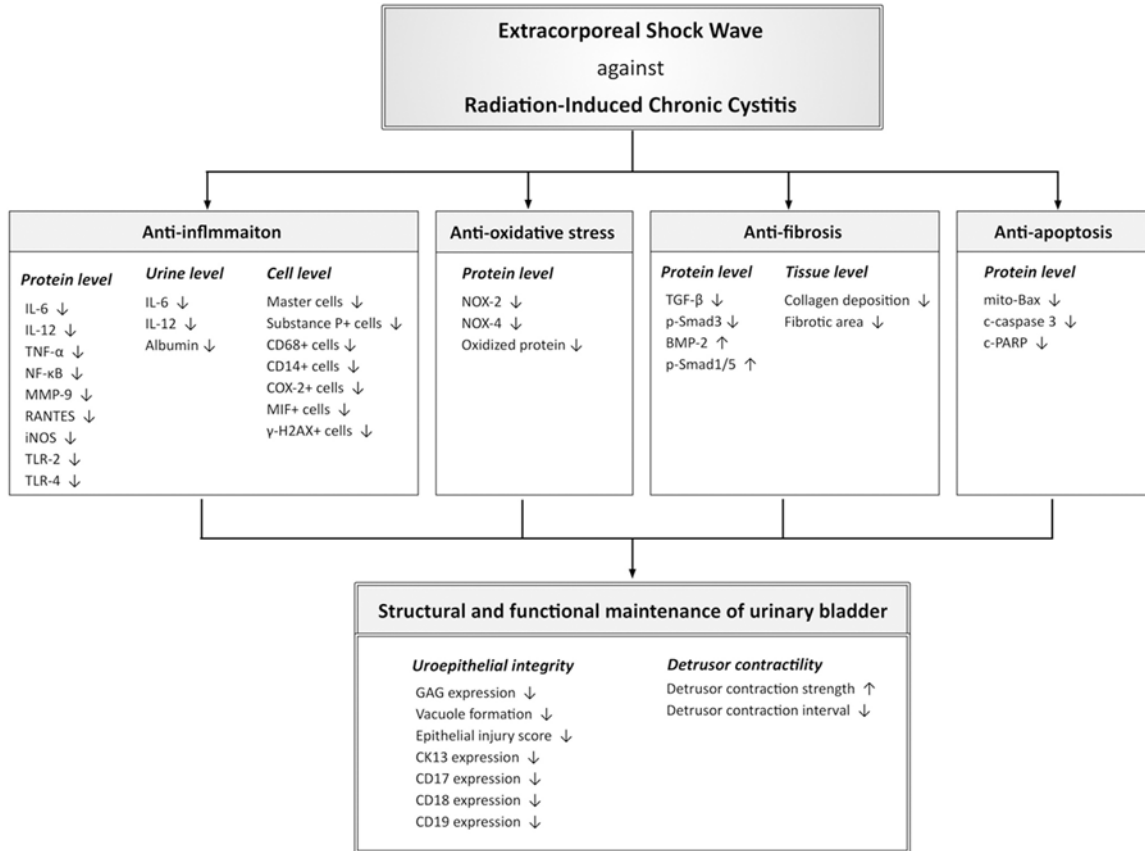
- [1] Stewart B and Wild C. World cancer report 2014. Lyon CEDEX, France. Chap 5.12. 465-481
- [2] Alesawi AM, El-Hakim A, Zorn KC and Saad F. Radiation-induced hemorrhagic cystitis. *Curr Opin Support Palliat Care* 2014; 8: 235-240.
- [3] Grellety T, Houede N, Hoepffner JL, Riviere J, Merino C, Lieutenant V, Gross-Goupil M, Richaud P, Dupin C, Sargos P and Roubaud G. Hemorrhagic cystitis in patients treated with cabazitaxel: a radiation recall syndrome? *Ann Oncol* 2014; 25: 1248-1249.
- [4] Mendenhall WM, Henderson RH, Costa JA, Hoppe BS, Dagan R, Bryant CM, Nichols RC, Williams CR, Harris SE and Mendenhall NP. Hemorrhagic radiation cystitis. *Am J Clin Oncol* 2015; 38: 331-336.
- [5] Payne H, Adamson A, Bahl A, Borwell J, Dodds D, Heath C, Huddart R, McMenemin R, Patel P, Peters JL and Thompson A. Chemical- and radiation-induced haemorrhagic cystitis: current treatments and challenges. *BJU Int* 2013; 112: 885-897.
- [6] Viswanathan AN, Lee LJ, Eswara JR, Horowitz NS, Konstantinopoulos PA, Mirabeau-Beale KL, Rose BS, von Keudell AG and Wo JY. Complications of pelvic radiation in patients treated for gynecologic malignancies. *Cancer* 2014; 120: 3870-3883.
- [7] Wit EM and Horenblas S. Urological complications after treatment of cervical cancer. *Nat Rev Urol* 2014; 11: 110-117.
- [8] Bonfili P, Franzese P, Marampon F, La Verghetta ME, Parente S, Cerasani M, Di Genova D, Mancini M, Vittorini F, Gravina GL, Ruggieri V, Di Staso M, Popov VM, Tombolini V and Di Cesare E. Intravesical instillations with polydeoxyribonucleotides reduce symptoms of radiation-induced cystitis in patients treated with radiotherapy for pelvic cancer: a pilot study. *Support Care Cancer* 2014; 22: 1155-1159.
- [9] Chong KT, Hampson NB and Corman JM. Early hyperbaric oxygen therapy improves outcome for radiation-induced hemorrhagic cystitis. *Urology* 2005; 65: 649-653.
- [10] Kaushik D, Teply BA and Hemstreet GP 3rd. Novel treatment strategy for refractory hemorrhagic cystitis following radiation treatment of genitourinary cancer: use of 980-nm diode laser. *Lasers Med Sci* 2012; 27: 1099-1102.
- [11] Linder BJ, Tarrell RF and Boorjian SA. Cystectomy for refractory hemorrhagic cystitis: contemporary etiology, presentation and outcomes. *J Urol* 2014; 192: 1687-1692.
- [12] Oliai C, Fisher B, Jani A, Wong M, Poli J, Brady LW and Komarnicky LT. Hyperbaric oxygen therapy for radiation-induced cystitis and proctitis. *Int J Radiat Oncol Biol Phys* 2012; 84: 733-740.
- [13] Rajaganapathy BR, Jayabalan N, Tyagi P, Kaufman J and Chancellor MB. Advances in therapeutic development for radiation cystitis. *Low Urin Tract Symptoms* 2014; 6: 1-10.
- [14] Shao Y, Lu GL and Shen ZJ. Comparison of intravesical hyaluronic acid instillation and hyperbaric oxygen in the treatment of radiation-induced hemorrhagic cystitis. *BJU Int* 2012; 109: 691-694.
- [15] Smit SG and Heyns CF. Management of radiation cystitis. *Nat Rev Urol* 2010; 7: 206-214.
- [16] Sommariva M, Lazzeri M, Abrate A, Guazzoni G, Sandri S and Montorsi F. Intravesical hyaluronic acid and chondroitin sulphate improve symptoms and quality of life in patients with late radiation tissue cystitis: an investigative pilot study. *Eur J Inflamm* 2014; 12: 177-185.
- [17] Tahir AR, Westhuyzen J, Dass J, Collins MK, Webb R, Hewitt S, Fon P and McKay M. Hyperbaric oxygen therapy for chronic radiation-induced tissue injuries: Australasia's largest study. *Asia Pac J Clin Oncol* 2015; 11: 68-77.
- [18] Talab SS, McDougal WS, Wu CL and Tabatabaei S. Mucosa-sparing, KTP laser coagulation of



## ECSW against radiation-induced chronic cystitis

- submucosal telangiectatic vessels in patients with radiation-induced cystitis: a novel approach. *Urology* 2014; 84: 478-483.
- [19] Vilar DG, Fadrique GG, Martin IJ, Aguado JM, Perello CG, Argente VG, Sanz MB and Gomez JG. Hyperbaric oxygen therapy for the management of hemorrhagic radio-induced cystitis. *Arch Esp Urol* 2011; 64: 869-874.
- [20] Chen YT, Yang CC, Sun CK, Chiang HJ, Chen YL, Sung PH, Zhen YY, Huang TH, Chang CL, Chen HH, Chang HW, Yip HK. Extracorporeal shock wave therapy ameliorates cyclophosphamide-induced rat acute interstitial cystitis through inhibiting inflammation and oxidative stress-in vitro and in vivo experiment studies. *Am J Transl Res* 2014; 6: 631-48.
- [21] Kabisch S and Fahlenkamp D. ESWT: interstitial cystitis-new promising indication for extracorporeal shock wave therapy. *Urology*. Level10 Buchverlag, Heilbronn 2013; 124-127.
- [22] Sheu JJ, Lee FY, Yuen CM, Chen YL, Huang TH, Chua S, Chen YL, Chen CH, Chai HT, Sung PH, Chang HW, Sun CK, Yip HK. Combined therapy with shock wave and autologous bone marrow-derived mesenchymal stem cells alleviates left ventricular dysfunction and remodeling through inhibiting inflammatory stimuli, oxidative stress & enhancing angiogenesis in a swine myocardial infarction model. *Int J Cardiol* 2015; 193: 69-83.
- [23] Chen KH, Yang CH, Wallace CG, Lin CR, Liu CK, Yin TC, Huang TH, Chen YL, Sun CK and Yip HK. Combination therapy with extracorporeal shock wave and melatonin markedly attenuated neuropathic pain in rat. *Am J Transl Res* 2017; 9: 4593-4606.
- [24] Chen YL, Chen KH, Yin TC, Huang TH, Yuen CM, Chung SY, Sung PH, Tong MS, Chen CH, Chang HW, Lin KC, Ko SF, Yip HK. Extracorporeal shock wave therapy effectively prevented diabetic neuropathy. *Am J Transl Res* 2015; 7: 2543-60.
- [25] Fu M, Sun CK, Lin YC, Wang CJ, Wu CJ, Ko SF, Chua S, Sheu JJ, Chiang CH and Shao PL. Extracorporeal shock wave therapy reverses ischemia-related left ventricular dysfunction and remodeling: molecular-cellular and functional assessment. *PLoS One* 2011; 6: e24342.
- [26] Wang CJ, Wang FS, Yang KD, Weng LH and Ko JY. Long-term results of extracorporeal shockwave treatment for plantar fasciitis. *Am J Sports Med* 2006; 34: 592-596.
- [27] Yeh KH, Sheu JJ, Lin YC, Sun CK, Chang LT, Kao YH, Yen CH, Shao PL, Tsai TH, Chen YL, Chua S, Leu S, Yip HK. Benefit of combined extracorporeal shock wave and bone marrow-derived endothelial progenitor cells in protection against critical limb ischemia in rats. *Crit Care Med* 2012; 40: 169-177.
- [28] Yuen CM, Chung SY, Tsai TH, Sung PH, Huang TH, Chen YL, Chen YL, Chai HT, Zhen YY, Chang MW, Wang CJ, Chang HW, Sun CK, Yip HK. Extracorporeal shock wave effectively attenuates brain infarct volume and improves neurological function in rat after acute ischemic stroke. *Am J Transl Res* 2015; 7: 976-94.
- [29] Chen YT, Chiang HJ, Chen CH, Sung PH, Lee FY, Tsai TH, Chang CL, Chen HH, Sun CK, Leu S, Chang HW, Yang CC, Yip HK. Melatonin treatment further improves adipose-derived mesenchymal stem cell therapy for acute interstitial cystitis in rat. *J Pineal Res* 2014; 57: 248-261.
- [30] Sun CK, Lee FY, Kao YH, Chiang HJ, Sung PH, Tsai TH, Lin YC, Leu S, Wu YC, Lu HI, Chen YL, Chung SY, Su HL, Yip HK. Systemic combined melatonin-mitochondria treatment improves acute respiratory distress syndrome in the rat. *J Pineal Res* 2015; 58: 137-150.
- [31] Sugaya K, Nishijima S, Kadekawa K, Ashitomi K, Ueda T and Yamamoto H. Naftopidil improves locomotor activity and urinary frequency in rats with pelvic venous congestion. *Biomed Res* 2016; 37: 221-226.

# ECSW against radiation-induced chronic cystitis



**Supplementary Figure 1.** Proposed mechanisms underlying the positive therapeutic effects of ECSW on reversing the deterioration of bladder function from radiotherapy-induced chronic cystitis. ECSW = extracorporeal shock wave; LEVF = left ventricular ejection fraction; TNF-α = tumor necrosis factor alpha; NF-κB = nuclear factor-κB; MMP-9 = matrix metalloproteinase 9; iNOS = inducible nitric oxide synthase; HO-1 = heme oxygenase 1; TGF-β = transforming growth factor beta; c-PARP = cleaved Poly (ADP-ribose) polymerase.